

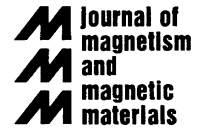


ELSEVIER

Available online at www.sciencedirect.com

SCIENCE @ DIRECT®

Journal of Magnetism and Magnetic Materials 260 (2003) 406–414

www.elsevier.com/locate/jmmm

Enhanced magnetic properties of Nd–Fe–B thin films crystallized by heat treatment

L.K.E.B. Serrona^{a,*}, R. Fujisaki^a, A. Sugimura^a, T. Okuda^a, N. Adachi^a,
H. Ohsato^a, I. Sakamoto^a, A. Nakanishi^{b,2}, M. Motokawa^c, D.H. Ping^d, K. Hono^d

^aDepartment of Materials Science and Engineering, Nagoya Institute of Technology, Gokiso-cho, Showa-ku, Nagoya 466-8555 Japan

^bSumitomo Special Metals Co., Shimamoto-cho, Osaka 618-0013 Japan

^cInstitute for Materials Research, Tohoku University, Sendai 980-8577 Japan

^dNational Institute for Materials Science, Sengen, Tsukuba 305-0047, Japan

Received 20 August 2002

Abstract

Nd₂Fe₁₄B Φ phase crystallites were formed in Nd_{16.7}Fe_{65.5}B_{17.8} thin films prepared by RF sputtering with subsequent heat treatment. The 2 μ m-thick films were deposited onto 0.1 mm Mo sheets at an average substrate temperature (T_s) of 365°C. The enhanced magnetic properties of the magnetically anisotropic thin films were investigated using different heating rates (h_r) of 10°C, 20°C, 50°C and 100°C/min in an annealing experiment. Transformation from the amorphous phase to the crystalline phase is clearly manifested by the formation of fine crystallites embedded as a columnar matrix of Nd₂Fe₁₄B phase. High-resolution scanning electron microscope data of the cross-section of the annealed films show columnar stacking of Nd₂Fe₁₄B crystallites with sizes <500 nm. Transmission electron microscope observations revealed that the microstructure of these films having out-of-plane magnetization consists of uniformly distributed Φ phase with grain size around 400 nm together with small Nd rich particles. This grain size of Φ phase is comparable to the single domain particle diameter of Nd₂Fe₁₄B. Significant change in iH_c , $4\pi M_{r\perp}$ and $4\pi M_{s\perp}$ with h_r was confirmed. Annealing conditions with a heating rate of 50°C/min to an annealing temperature (T_a) of 650°C for 30 min was consequently found to give optimum properties for the NdFeB thin films. The resulting magnetic properties, considered to be the effect of varying h_r were $iH_c = 1307$ – 1357 kA/m, $4\pi M_{r\perp} = 0.78$ – 1.06 T and $4\pi M_{s\perp} = 0.81$ – 1.07 T.

© 2002 Elsevier Science B.V. All rights reserved.

Keywords: Nd₂Fe₁₄B; Thin films; High coercivity; Thermal annealing; Microstructure; Heating rate; Hard magnetic materials

1. Introduction

NdFeB permanent magnet thin films are ideal for micro-motors, micro-actuators [1], micro-electromechanical systems [2], magnetic sensors, etc., due to its remarkable room temperature intrinsic properties, which include high magnetization and high magneto-crystalline anisotropy [3].

*Corresponding author. Tel.: +81-52-735-5290; fax: +81-52-735-5294.

E-mail address: leokebs@hotmail.com (L.K.E.B. Serrona).

¹On leave from the Department of MSE, University of the Philippines-Diliman, Diliman, Quezon City 1101, Philippines.

²Present Address: Takuma National College of Technology, Takuma-cho, Mitoyo-gun, Kagawa 769-1192, Japan.

These magnetic properties when associated with textured NdFeB Φ phase crystallites with the c -axis preferentially aligned along the film normal, an excellent material for permanent magnet thin film applications can be realized. Reasonably, a major concern in the preparation of Nd₂Fe₁₄B materials in nanocrystalline form is to take advantage of the high magnetocrystalline anisotropy of NdFeB Φ phase achieved when an optimal nanocrystalline structure is formed. Recently, our experiments yielded significant results in the fabrication of these magnetic thin films by sputtering the amorphous films onto Mo substrates with subsequent vacuum annealing to crystallize the films. We were able to optimize some important parameters like target composition which would give higher coercivity and vacuum annealing conditions such as temperature and time for crystallization [4,5]. In another related experiment, the use of glass insulation between the substrate and the water-cooled substrate holder made it possible to keep the surface temperature of the substrate during deposition at a certain range below the crystallization temperature and far above room temperature [6]. Amorphous films deposited in HTD conditions (glass-insulated Mo substrates) exhibited weak perpendicular anisotropy that were deemed necessary for the self-texturing mechanism in the Φ phase crystallites in annealed films. On the contrary, one deposited in LTD conditions (no glass insulation) exhibited typical soft magnetic properties with in-plane anisotropy. Investigating further on post-annealing conditions, it was found that aside from using the initial heating rate (h_r) of 10°C/min which produced anisotropic films with $iH_c \sim 1290$ kA/m [6], higher h_r in vacuum annealing was also effective in producing enhanced magnetic properties.

Using a lamp heating type vacuum furnace, the experiment was conducted based on the rapid thermal annealing (RTA) techniques that involves a time–temperature profile characterized by quick heating (high ramp rate) and very short annealing time. The RTA method has been reported to be essential in the fabrication of isotropic nanostructured NdFeB films with high H_c and high (M_r/M_s) ratio [7]. In addition, according to experimental

results in nanocomposite magnets, rapid annealing enhances the homogeneity of the magnetic phases thus increasing the exchange-coupled regions between the interacting grains [8]. We annealed the films for 30 min and a maximum h_r of 100°C/min and these parameters are actually incomparable with the heating rate of 200°C/s and 10 s annealing time for RTA. However, comparing our annealing techniques with RTA procedures, there exist certain similar effects particularly in the development of the microstructure corresponding to enhanced magnetic properties.

Similar phenomena in melt quench ribbons were found wherein direct quenching led to isotropic crystal growth [9]. Whereas, we found out that our thermal annealing procedure in Nd–Fe–B thin films prepared in HTD conditions resulted to anisotropic crystal growth. In both cases, high coercivity is developed by the suppression of crystal growth into appropriate grain size as an effect of the different heat treatment parameters. In melt quench ribbons, high magnetization is due to the exchange coupling in the nanocrystals with grains size much lesser than the single domain particle diameter of 260 nm for Nd₂Fe₁₄B [10]. It is also characterized by the homogeneous distribution of regularly shaped grains. On the other hand, our work on Nd–Fe–B thin films using typical thermal annealing with an optimum heating rate of 50°C/min and annealing at 650°C for 30 min led to the development of high coercivity films with out-of-plane magnetization and columnar grain structure observed in the film cross-section. The anisotropic crystal growth of Φ phase grains resulted to nearly single domain size particles having a texture with the c -axis preferentially oriented along the film normal. High coercivity (iH_c) and high remanent to saturation magnetization ratio (M_r/M_s) were also found.

Present work was aimed to examine the effect of increasing the initial heating rate of vacuum thermal annealing on the microstructural and magnetic properties in the thin film samples. In this paper, we will report on the development of desirable hard magnetic properties from film samples which are amorphous as deposited and were subsequently crystallized based on optimum parameters of a post annealing method.

2. Experimental procedure

The NdFeB films were deposited using a conventional RF sputtering device with a 100 mm diameter cast $\text{Nd}_{20}\text{Fe}_{64}\text{B}_{16}$ target [4] added with a $(1.5\text{ cm})^2$ Fe sheet. The working distance between substrate and target is 50 mm. The sputtering chamber was evacuated to a background pressure of about 2.7×10^{-4} Pa and then Ar gas was introduced into the chamber and all deposition was made at a constant total pressure of 6.7×10^{-1} Pa. The films were deposited on ultrasonically pre-cleaned and chemically etched 0.1 mm thick as-rolled Mo sheets. The Mo substrates were thermally insulated by 1 mm glass sheet from a water-cooled copper substrate holder. The details about the use of glass insulation beneath the substrates in this experiment is reported elsewhere [6]. The junction of the alumel–chromel thermocouple was inserted between the substrate and glass insulation for monitoring the temperature of the substrate in the entire deposition process. The films were deposited for 1 h at a rate of around $260 \text{ \AA}/\text{min}$ with an RF power = 350 W. No in situ heating and biasing magnetic field were employed. After film deposition, a thin coating of Ti around 700 \AA was deposited for 5 min at 350 W to protect the film surface from oxidation. Annealing, shown schematically in Fig. 1 was done in vacuum using an infrared image-furnace. In previous reports, the typical conditions for initial heating rate (h_r), maximum temperature (T_a) and holding time (t_a)

were $10^\circ\text{C}/\text{min}$, 650°C and 30 min, respectively. The specimens were furnace-cooled to room temperature. These were experimentally optimized for the films prepared using $\text{Nd}_{20}\text{Fe}_{64}\text{B}_{16}$ target [6]. To determine the optimum initial heating rate (h_r) that will supposedly correspond to high iH_c , $4\pi M_{r\perp}$ and $4\pi M_{s\perp}$ values, a series of annealing experiments were performed using $h_r = 10^\circ\text{C}$, 20°C , 50°C and $100^\circ\text{C}/\text{min}$. DEKTAK profile meter was used to measure the thickness of the film samples. SQUID Measurements and X-ray diffraction techniques were used to characterize the magnetic and structural properties of the crystalline films, respectively. Cross-section morphologies and planar grain sizes were examined by high-resolution SEM and TEM, respectively. The composition of the films was analyzed by inductively coupled plasma (ICP) method.

3. Results and discussion

3.1. XRD patterns

During RF sputter deposition of the film in the HTD conditions, the substrate temperature changed from 350°C to 373°C . The average temperature for the entire deposition is 365°C . As can be seen in Fig. 2, the as deposited film is amorphous with a diffraction peak identified as Ti (00.2) and two other peaks indexed as Mo(110) and Mo(200). Heating rate (h_r) dependence of the X-ray diffraction patterns for the annealed films measured with $\text{Cu K}\alpha$ radiation is also presented in Fig. 2. The phase identification and determination of crystallographic parameters were based on the tetragonal $\text{Nd}_2\text{Fe}_{14}\text{B}$ (JCPDS 39-0473) data. It is obvious that the c -axis is strongly oriented perpendicular to the film plane because the 002 ℓ peaks such as the 004, 006 and 008 reflections of the Φ phase have considerably high intensity. In addition to the 110 and 200 diffraction peaks of Mo substrates, there are two unknown small peaks and Nd oxide diffraction peaks observed at $2\theta = 30.4^\circ$ and 53.5° . Other Φ phase peaks like 214, 115, 225, 208 and 218 are also observed but their intensities are very weak. The XRD patterns show no extra phase developed during annealing

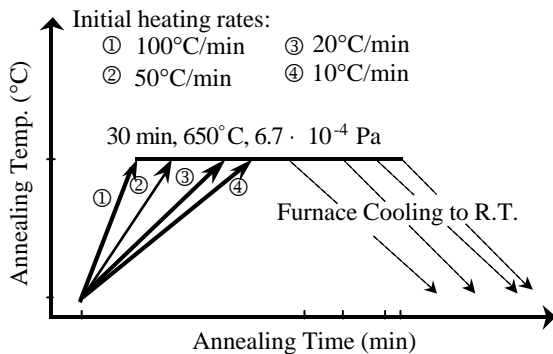


Fig. 1. Schematic representation of the annealing procedure used in the experiment.

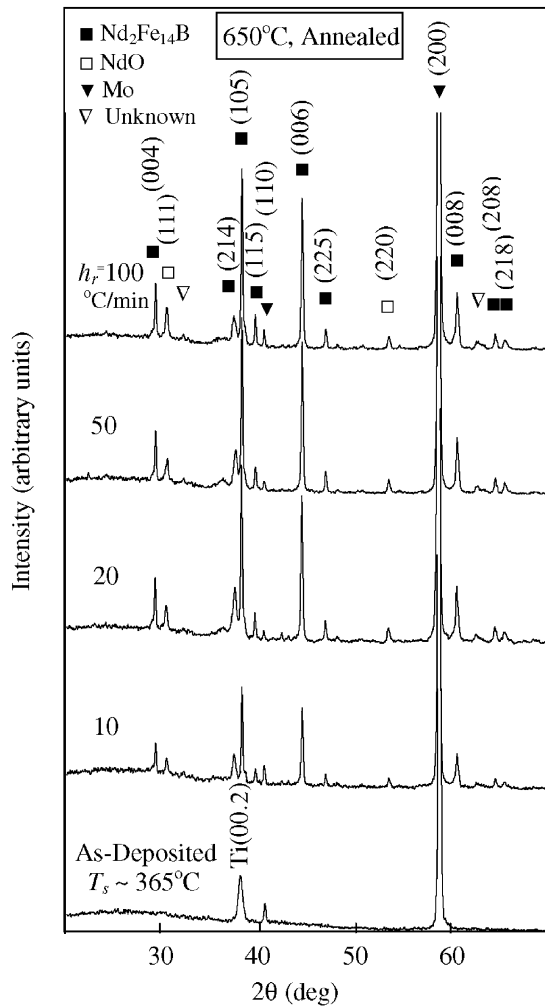


Fig. 2. X-ray diffraction patterns of as-deposited film and annealed films plotted in increasing order of the initial heating rates (h_r).

using h_r up to $100^\circ\text{C}/\text{min}$. This kind of texturing has been consistently considered in previous experiments to be an indication of remarkable orientation of c -axis perpendicular to the film plane [11].

A plot of the intensity ratio between the strong diffraction line 006 and 214 (I_{006}/I_{214}) and h_r is made to compare the perpendicular orientation of the crystalline phases. The 214 diffraction index was chosen because it has the strongest intensity among the powder diffraction peaks from Φ phase

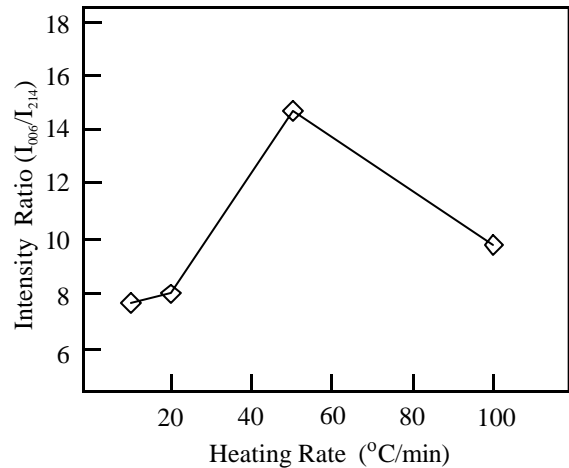


Fig. 3. Relative intensity ratio of (I_{006}/I_{214}) as a function of the initial heating rates during annealing.

and represents diffraction planes that tend to orient the crystals away from the normal to the film plane direction. For the isotropic NdFeB powder material, I_{006}/I_{214} ratio is around 0.28 [12]. Fig. 3 depicts the profile of the intensity ratios and initial heating rates having a maximum value at $h_r = 50^\circ\text{C}/\text{min}$ and a minimum value at $h_r = 10^\circ\text{C}/\text{min}$. Higher values for the I_{006}/I_{214} intensity ratio indicate that the film samples possess considerable degree of orientation perpendicular to the film plane. The identical profiles of the h_r and magnetization curves in Figs. 3 and 5, respectively, proves existence of the influence of h_r on the texturing of the films. The close relationship between texture and $4\pi M_\perp$ can therefore be established.

3.2. Magnetic hysteresis loops

Shown in Fig. 4(a) and (b) are the hysteresis loops measured with field applied up to $5600\text{ kA}/\text{m}$ in the directions perpendicular (H_\perp) and parallel (H_\parallel) to the film plane using SQUID magnetometer. For the films measured with H_\perp , higher c -axis texturing are indicated by higher $4\pi M_{r\perp}$ and $4\pi M_{s\perp}$ values. The hysteresis loops of the films reveal a common single magnetic phase characteristics although there are secondary phases present. According to the results summarized in Fig. 5, the

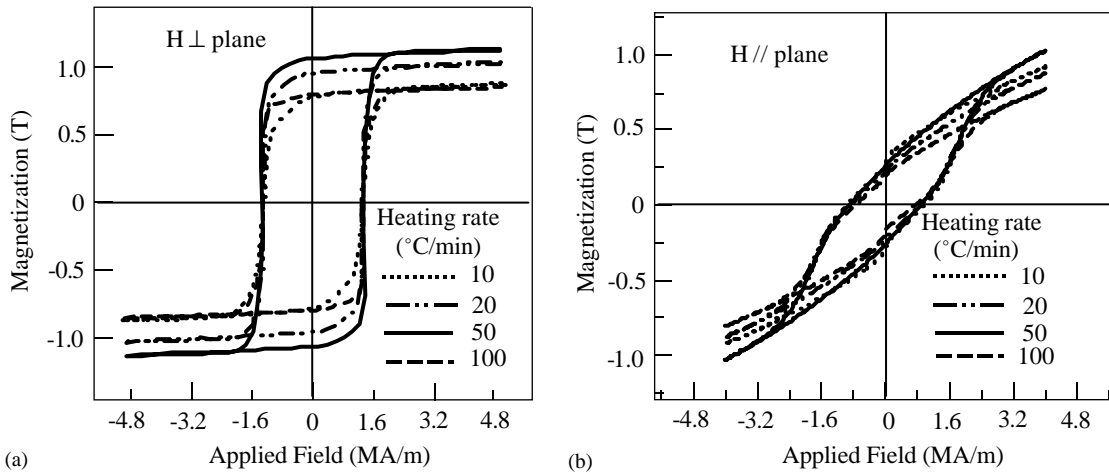


Fig. 4. Hysteresis loops of films annealed using different initial heating rates. (a) Applied field is normal to the film surface. Correction for demagnetization was made. (b) Applied field is along the film plane.

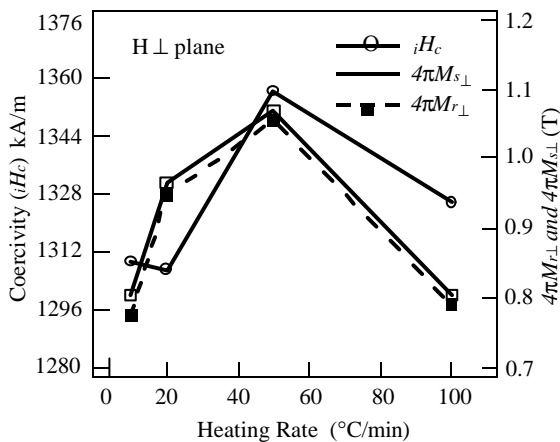


Fig. 5. Dependence of the intrinsic coercivity (iH_c), remanent ($4\pi M_{r\perp}$) and saturation magnetization ($4\pi M_{s\perp}$) on the initial heating rates (h_r).

optimum initial heating rate is around 50 °C/min higher than the usual 10 °C/min used in previous experiments [6,11]. The $4\pi M_{r\perp}$ and $4\pi M_{s\perp}$ of the film annealed using $h_r = 50$ °C/min is higher than those films annealed using $h_r = 10$ °C, 20 °C and 100 °C/min. Samples annealed using either lower h_r (10 °C/min and 20 °C/min) or higher h_r (100 °C/min) than the optimum is characterized by low coercivity and low magnetization. The small but noticeable changes in iH_c values are indications of

the existence of minor changes in size and shape of Φ phase crystallites. Although there is no important change in the coercivity mechanism, it is obvious that c -axis texturing of the films affected the iH_c values. Significant results can also be found in the high squareness of the loops, which is nearly unity (~ 1).

Magnetic properties measured with H_{\parallel} , out-of-plane magnetization behavior is observed. Small bends near $H = 0$ kA/m are present except for the condition where $h_r = 50$ °C/min. These are caused by the presence of small quantities of soft magnetic phases with in-plane anisotropy and these were actually undetectable by conventional X-ray measurements. It can also be observed that hysteresis loops appear long and narrow with an obvious change in its inclinations towards saturation as h_r is varied. The changes in the slopes can be regarded as an effect of the different texture in the films.

The hysteresis loops measured with H_{\perp} and H_{\parallel} illustrate that the Φ phase crystallites formed in the annealed films indicate that the c -axis is parallel to the film normal and randomly oriented along the film plane after a magnetic field was applied perpendicular and parallel to the film surface, respectively. The combined high magnetocrystalline anisotropy and high saturation magnetization

in the $\text{Nd}_2\text{Fe}_{14}\text{B}$ phase contributed to the development of the anisotropic behavior in the films. Enhanced magnetic properties resulted from the microstructural transformations during annealing that were affected by the changes in the initial heating rates directly related to the extent of the nucleation and crystallization process.

3.3. SEM micrographs

Fig. 6 shows the SEM micrographs of the cross-section of amorphous and annealed Nd–Fe–B thin films using two different h_r of 10°C and $50^\circ\text{C}/\text{min}$. Amorphous films surface are mirror-like and the cross-section surface are dense and continuous and no voids are found as shown in Fig. 6(a). Subsequent annealing transforms the films into a stack of microcrystalline grains with diameters $< 500\text{ nm}$ in a columnar structure together with some voids considered to be a source of the anisotropic character which in turn influences the magnetic anisotropy in this films [13]. The crystallites are arranged along a direction perpendicular to the film surface closely associated with the direction of the growth of the film during sputtering deposition. Micrographs in Fig. 6(b) and (c) correspond to an assembly of small crystallites less than a micron size comprising the microscopic texture of the permanent magnet material. However, intrinsic magnetic properties are actually dependent on size of the individual grains and the presence of appropriate grain boundary phases [14].

The micrograph for $h_r = 10^\circ\text{C}/\text{min}$ reveals that this film consists of $\text{Nd}_2\text{Fe}_{14}\text{B}$ nanocrystallites less than $0.5\ \mu\text{m}$ in diameter. The cross-section is characterized by some regularly spaced blocks as well as voids formed in a columnar-like structure. At this heating rate, films produced have lesser coercivity and remanent magnetization compared to the films annealed at $h_r = 20^\circ\text{C}$ and $50^\circ\text{C}/\text{min}$. At an optimum $h_r = 50^\circ\text{C}/\text{min}$, the film cross-section is characterized by the presence of more finer crystals with diameters less than $0.3\ \mu\text{m}$. These fine crystals together with some small voids surround the large and elongated $0.5\ \mu\text{m}$ crystallites. Enhanced magnetic properties were found in this sample with $iH_c = 1357\ \text{kA}/\text{m}$, $4\pi M_{r\perp} = 1.06\ \text{T}$

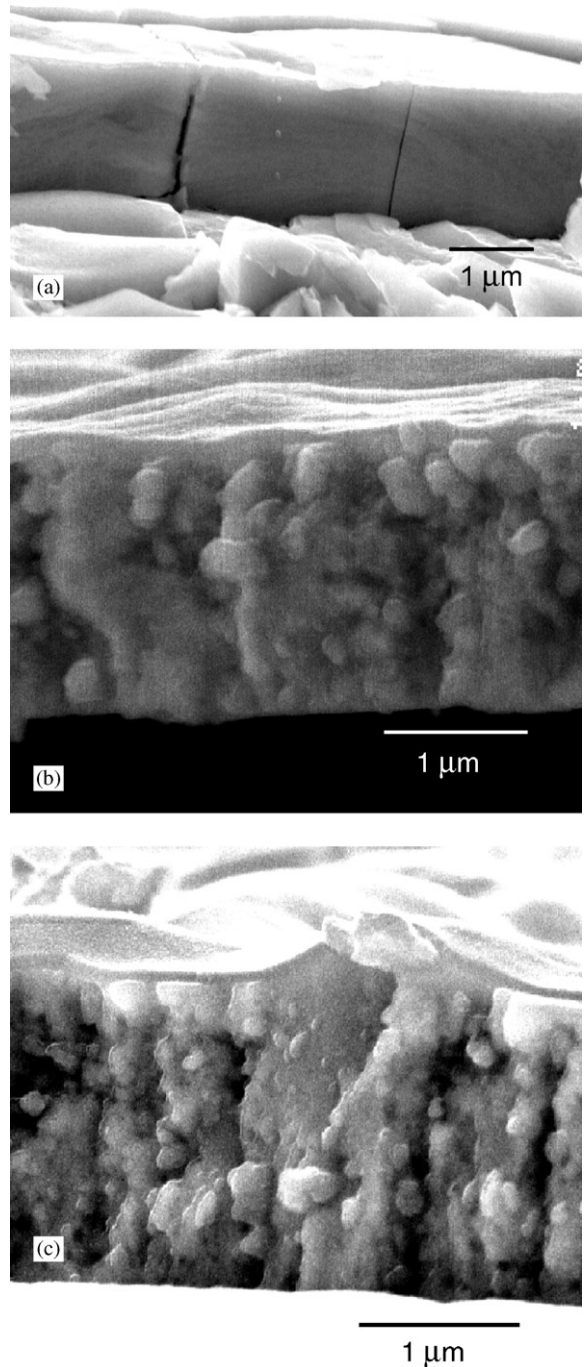


Fig. 6. Cross-sectional SEM micrographs showing the morphology of NdFeB films at (a) as-deposited state, (b) $h_r = 10^\circ\text{C}/\text{min}$ and (c) $h_r = 50^\circ\text{C}/\text{min}$.

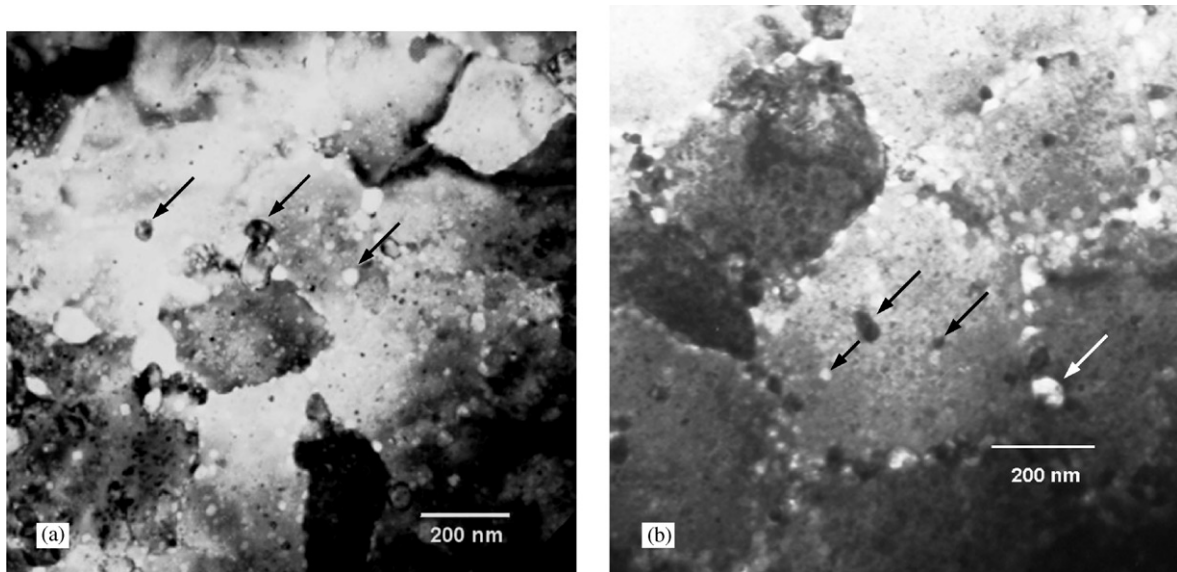


Fig. 7. Planar TEM images of annealed films (650°C, 30 min) with h_r 10°C/min and; (b) 50°C/min. Small arrow points to the location and Nd rich particles (white and dark spots).

and $4\pi M_{s\perp} = 1.07$ T. Distinct cross-sectional microstructure can be observed from the two micrographs with h_r of 10°C and 50°C/min. This can be due to the effect of different crystallization behavior brought about by the use of different h_r . It can also be seen that the columnar alignment and homogeneous distribution of the crystallites can be understood to be a source of the high coercivity and anisotropic behavior inherent in the films.

3.4. TEM micrographs

The microstructure of this off-stoichiometric $\text{Nd}_{16.7}\text{Fe}_{65.5}\text{B}_{17.8}$ thin film consists of large and equiaxed grains having the hard magnetic phase surrounded by minor Nd rich particles. Fig. 7(a) and (b) show the bright field TEM images of the films annealed at 650°C for 30 min using $h_r = 10^\circ\text{C}$ and 50°C/min, respectively. From the micrographs, Nd rich particles and other small precipitates (indicated by small arrows) are present in the grain boundaries and there are few particles found inside the grains. The grain size for this highly anisotropic Nd–Fe–B thin film material estimated from the micrographs is around 400 nm.

This grain size is much greater than the single domain size of ~ 160 nm of melt spun ribbons [15] with nearly the same coercive force and Curie temperature. Critical single domain particle diameters for $\text{Nd}_2\text{Fe}_{14}\text{B}$ of 300 and 400 nm were actually reported earlier by Herbst et.al. [16] and Livingston, [17] respectively. However, recent studies reported grain sizes around 50 nm or less corresponding to enhanced magnetic properties for both isotropic and anisotropic Nd–Fe–B nanocrystalline materials [14]. In the case of highly coercive and anisotropic sputtered films, Kapitnov et.al. [18] reported grain sizes < 600 nm. They observed Nd–Fe–B grain structures with small inclusions in and out of the individual grains. The initial magnetization curve of the film annealed using $h_r = 10^\circ\text{C}/\text{min}$ behaved like typical nucleation type permanent magnet [11]. Therefore, it is reasonable to consider that the grains observed in our annealed film can be regarded as single domain particles.

Slow initial heating rate at 10°C/min favors growth of other minority phases including some voids that would lead to the formation of inhomogeneous microstructure. It can be observed from Fig. 7(a) that the irregular form

and distribution of the grains maybe a consequence of prolonged initial heating. Corresponding iH_c and $4\pi M_{r\perp}$ for this sample is 1309 kA/m and 0.78 T, respectively. On the other hand, for $h_r = 50^\circ\text{C}/\text{min}$, well-defined grain patterns are observable in Fig. 7(b) with few smaller particles inside and around the $\text{Nd}_2\text{Fe}_{14}\text{B}$ grains. The quick increase in heating suppressed the growth of various intergranular phases giving way to the $\text{Nd}_2\text{Fe}_{14}\text{B}$ phase to form a fine-grained microstructure. For intermediate and higher h_r at 20°C and $100^\circ\text{C}/\text{min}$, respectively, the effects were not remarkable to gain consideration because experimental results showed inadequate description for the comparison of the magnetic and structural properties.

Even though it is shown in Fig. 4(a) that the squareness ratio of all the loops is nearly unity (~ 1) after correction of the demagnetizing field, there exist some remarkable changes in $4\pi M_{r\perp}$ and $4\pi M_{s\perp}$ values as shown in Fig. 5. Identical film samples were previously reported to contain single magnetic phase [6] and in this recent investigation, magnetic property changes were found to be associated with the formation and distribution of $\text{Nd}_2\text{Fe}_{14}\text{B}$ grains as shown in Fig. 7(a) and (b). From Fig. 7(a), non-uniform grains structure formed using $h_r = 10^\circ\text{C}/\text{min}$ resulted to an entirely weaker exchange interaction between neighboring $\text{Nd}_2\text{Fe}_{14}\text{B}$ nanocrystallites suggesting lower magnetization. Examining the results for $h_r = 50^\circ\text{C}/\text{min}$ shown in Fig. 7(b), a stronger exchange coupling among the nanocrystallites are to be expected because of the formation of a fine-grained structure. In that case, increased exchange interaction between the magnetic grains resulted to higher magnetization [19].

4. Conclusions

The synthesis of anisotropic and high coercivity NdFeB thin films by post annealing of as RF-sputter-deposited films has been discussed with emphasis on the enhancement of magnetic properties due to the optimized initial heating rate in the thermal annealing experiment. The films deposited at an average substrate temperature of 365°C were amorphous and were subsequently annealed in

vacuum at 650°C for 30 min. All the film samples show remarkable structural and magnetic properties in its crystalline form after annealing using different h_r of 10°C , 20°C , 50°C and $100^\circ\text{C}/\text{min}$. Two distinct results between using 10 and $50^\circ\text{C}/\text{min}$ heating rates showed formation of $\text{Nd}_2\text{Fe}_{14}\text{B}$ nanocrystals in the columnar cross-section of the film with diameters $<0.5\ \mu\text{m}$ and $<0.3\ \mu\text{m}$, respectively. The increase of iH_c and $4\pi M_{r\perp}$ to 1357 kA/m and 1.06 T, respectively, made it possible for the thin film sample to attain remarkable magnetic properties at an h_r of $50^\circ\text{C}/\text{min}$. The $\text{Nd}_2\text{Fe}_{14}\text{B}$ grain size after subsequent annealing is estimated to be about 400 nm from TEM observations. Crystallization at higher initial heating rates produced higher density of nuclei that resulted to finer microstructure and suppressed formation of possible low temperature phases. The resulting nanocrystalline structure showed some indication in the magnetic properties of exchange interaction between the magnetic moments of the $\text{Nd}_2\text{Fe}_{14}\text{B}$ individual grains. These are believed to have contributed to the high iH_c , $4\pi M_{r\perp}$ and $4\pi M_{s\perp}$ values. It can be summarized therefore, that the enhancement of remanence accompanied by the increase in coercivity is obtained from crystallizing amorphous films into nearly single domain $\text{Nd}_2\text{Fe}_{14}\text{B}$ nanocrystallites characterized by a c -axis oriented textured structure developed normal to the film plane. These results are very important for the understanding of high coercivity mechanism and then for the selection of the best possible microstructural characteristic to be controlled in order to further improve the magnetic properties of the films.

Acknowledgements

The authors are thankful to Dr. T. Hihara of the Nagoya Institute of Technology (NIT) and Mr. M. Sakai of the Okazaki National Research Institute for the SQUID measurements and to Prof. T. Kasuga (NIT) for the Scanning Electron Microscopy observations. L.K.E.B. Serrona gratefully acknowledges of the support of

the Japanese Government Monbu-kagakusho scholarship.

References

- [1] S. Yamashita, J. Yamasaki, M. Ikeda, N. Iwabuchi, J. Appl. Phys. 70 (1991) 6627; H. Lemke, T. Lang, T. Göddenhenrich, C. Heiden, J. Magn. Magn. Mater. 148 (1995) 426.
- [2] T.S. Chin, J. Magn. Magn. Mater. 209 (2000) 75.
- [3] R.A. McCurrie, *Ferromagnetic Materials: Structure and Properties*, Academic Press Ltd., London, 1994.
- [4] A. Nakanishi, M. Ueda, T. Okuda, N. Mizutani, J. Nishiyama, M. Motokawa, Z. Wang, N. Adachi, H. Ohsato, J. Magn. Magn. Mater. 196–197 (1999) 295.
- [5] N. Mizutani, T. Okuda, A. Nakanishi, J. Nishiyama, M. Motokawa, Z. Wang, N. Adachi, H. Ohsato, J. Magn. Soc. Japan 297 (1999) 23.
- [6] L.K.E.B. Serrona, A. Sugimura, R. Fujisaki, T. Okuda, N. Adachi, H. Ohsato, I. Sakamoto, A. Nakanishi, M. Motokawa, *Trans. Magn. Soc. Japan* 2 (2002) 93.
- [7] M. Yu, Y. Liu, S.H. Liou, D.J. Sellmyer, J. Appl. Phys. 83 (1998) 6611.
- [8] A. Kojima, A. Makino, A. Inoue, J. Appl. Phys. 87 (2000) 6576.
- [9] L. Withanawasam, G.C. Hadjipanayis, R.F. Krause, J. Appl. Phys. 75 (1994) 6646.
- [10] D. Jiles, *Introduction to Magnetism and Magnetic Materials*, Chapman and Hall, New York, 1991.
- [11] K. Terazawa, L. Serrona, T. Okuda, N. Adachi, I. Sakamoto, A. Nakanishi, in: H. Kaneko, M. Homma, M. Okada (Eds.), *Proceedings of the 16th International Workshop on Rare Earth Magnets and Their Applications*, Sendai, 2000, pp. 393–402 (The Japan Institute of Metals, Japan, 2000).
- [12] Powder Diffraction File, JCPDS ICDD, PA, USA, 1989.
- [13] J.A. Thornton, J. Vac. Sci. Technol. A 4 (1986) 63059.
- [14] G.C. Hadjipanayis, J. Magn. Magn. Mater. 200 (1999) 373.
- [15] J.J. Croat, J.F. Herbst, R.W. Lee, F.E. Pinkerton, J. Appl. Phys. 55 (1984) 2078.
- [16] J.F. Herbst, *Rev. Mod. Phys.* 63 (1991) 819.
- [17] J.D. Livingston, *Proceedings of the 8th International Workshop on Rare-Earth Magnets and their Applications*, Dayton, OH, 1985.
- [18] B.A. Kapitanov, N.V. Kornilov, Ya.L. Linetsky, V.Yu. Tsvetkov, J. Magn. Magn. Mater. 127 (1993) 289.
- [19] M. Dahlgren, R. Grösingger, in: F.P. Missel (Ed.), *Materials Science Forum*, Vols. 302–303, Trans Tech Publications, Switzerland, 1999, p. 263.